or perpendicular to the radial direction (within the scattering plane) (corresponding to an ω scan),

$$L_{1\mathrm{D},\perp,\mathrm{per}} = (\alpha_2^2 + \alpha_1^2 + 4\eta_0' \tan^2\theta - 4\alpha_1'' \tan\theta)^{-1/2}(1/\cos\theta). \quad (4.2.8.7)$$

Note that only the radial scan yields a simple θ dependence ($\sim 1/\sin\theta$).

From these considerations it is recommended that integrated intensities from scans perpendicular to a diffuse plane or a diffuse streak should be used in order to extract the disorder cross sections. For other scan directions, which make an angle α with the intersection line (diffuse plane) or with a streak, the L factors are simply $L_{2\mathrm{D},\perp}/\sin\alpha$ and $L_{1\mathrm{D},\perp}/\sin\alpha$, respectively.

One point should be emphasized: since in a usual experiment with a single counter the integration is performed over an angle $\Delta\omega$ *via* a general $\delta\omega{:}(g\delta 2\theta)$ scan, an additional correction factor arises:

$$\Delta\omega/\Delta\mathbf{H}_\beta = \sin(\beta+\theta)/(\mathbf{k}_0 \sin 2\theta). \quad (4.2.8.8)$$

β is the angle between $\mathbf{H}_0$ and the scan direction $\mathbf{H}_\beta$, and $g = (\tan\beta + \tan\theta)/(2\tan\theta)$ defines the coupling ratio between the rotation of the crystal around a vertical axis and the rotation of the detector shaft. The so-called 1:2 and ω-scan techniques are most frequently used, where $\beta = 0$ and 90°, respectively.

White-beam techniques: Techniques for the measurement of diffuse scattering using a *white* spectrum are common in neutron diffraction. Owing to the relatively low velocity of thermal or cold neutrons, TOF methods in combination with time-resolving detector systems placed at a fixed angle 2θ allow for a simultaneous recording along a radial direction through the origin of reciprocal space (see, *e.g.*, Turberfield, 1970; Bauer *et al.*, 1975). The scan range is limited by the Ewald spheres corresponding to $\lambda_{\max}$ and $\lambda_{\min}$, respectively. With several such detector systems placed at different angles or a 2D detector several scans may be carried out simultaneously during one neutron pulse.

An analogue of neutron TOF diffractometry in the X-ray case is a combination of a white source of X-rays and an energy-dispersive detector. This technique, which has been known in principle for a long time, suffered from relatively weak white sources. With the development of high-power X-ray generators and synchrotron sources this method has now become highly interesting. Its use in diffuse-scattering work (in particular, the effects on resolution) is discussed by Harada *et al.* (1984).

Some examples of neutron instruments dedicated to diffuse scattering are the diffractometers D7 at the Institut Laue–Langevin (ILL, Grenoble), DNS at the Forschungsneutronenquelle Heinz Maier-Leibnitz (FRM-II, Munich), G4-4 at the Laboratoire Léon Brillouin (LLB, Saclay) or SXD at ISIS, Rutherford Appleton Laboratory (RAL, UK). The instrument DNS uses a polarization analysis for diffuse scattering (Schweika & Böni, 2001; Schweika, 2003) and the SXD diffractometer is a TOF instrument using a (pulsed) white beam (Keen & Nield, 2004). All these instruments are equipped with banks of detectors. The single-crystal diffractometer D19 at the ILL, equipped with a multiwire area detector, is also suitable for collecting diffuse data. The flat-cone machine E2 at the Hahn–Meitner Institut (HMI, Berlin) is equipped with a bank of area detectors, has an option to record higher-order layers and can also be operated in an 'elastic' mode with a multicrystal analyser. The instrument D10 at the ILL is a versatile instrument which can be operated as a low-background two-axis or three-axis diffractometer with several further options. Neutron diffractometers that have recently become operational are BIX-3 at the Japan Atomic Energy Research Institute (JAERI, Japan), LADI at the ILL, where neutron-sensitive IPs are used for macromolecular work (for a comparison see Niimura *et al.*, 2003), and RESI at the Forschungsneutronenquelle Heinz Maier-Leibnitz (FRM-II, Munich) for common solid-state investigations. Information about all these instruments can be found in the respective handbooks or on the websites of the facilities.

4.2.8.2. Powders and polycrystals

The diffuse background in powder diagrams also contains valuable information about disorder. Only in very simple cases can a model be deduced from a powder pattern alone, but a refinement of a known disorder model can favourably be carried out, *e.g.* the temperature dependence may be studied. On account of the intensity integration, the ratio of diffuse intensity to Bragg intensity is enhanced in a powder pattern. Moreover, a powder pattern contains, in principle, all the information about the sample and might thus reveal more than single-crystal work. However, in powder-diffractometer experiments preferred orientations and textures could lead to a complete misidentification of the problem. Single-crystal experiments are generally preferable in this respect. Nevertheless, high-resolution powder investigations may give quick supporting information, *e.g.* about superlattice peaks, split reflections, lattice strains, domain-size effects, lattice-constant changes related to a disorder effect *etc*.

Evaluation of diffuse-scattering data from powder diffraction follows the same theoretical formulae developed for the determination of the radial distribution function for glasses and liquids. The final formula for random distributions may be given as (Fender, 1973)

$$I_D^p = \{\langle|F(\mathbf{H})|^2\rangle - |\langle F(\mathbf{H})\rangle|^2\} \sum_i s_i \sin(2\pi H r_i)/(2\pi H r_i). \quad (4.2.8.9)$$

s_i represents the number of atoms at distance r_i from the origin. An equivalent expression for a substitutional binary alloy is

$$I_D^p = \alpha(1-\alpha)\{|f_2(\mathbf{H}) - f_2(\mathbf{H})|^2\} \sum_i s_i \sin(2\pi H r_i)/(2\pi H r_i). \quad (4.2.8.10)$$

A quantitative calculation of a diffuse background is also helpful in combination with Rietveld's method (1969) for refining an averaged structure by fitting Bragg data. In particular, for highly anisotropic diffuse phenomena characteristic asymmetric line shapes occur.

The calculation of these line shapes is treated in the literature, mostly neglecting the instrumental resolution (see, *e.g.*, Warren, 1941; Wilson, 1949; Jones, 1949; and de Courville-Brenasin *et al.*, 1981). This is not justified if the variation of the diffuse intensity becomes comparable with that of the resolution function, as is often the case in neutron diffraction. The instrumental resolution may be incorporated using the resolution function of a powder instrument (Caglioti *et al.*, 1958). A detailed analysis of diffuse peaks is given by Yessik *et al.* (1973) and the equivalent considerations for diffuse planes and streaks are discussed by Boysen (1985). The case of 3D random disorder (incoherent neutron scattering, monotonous Laue scattering, averaged TDS, multiple scattering or short-range-order modulations) is treated by Sabine & Clarke (1977).

In polycrystalline samples the cross section has to be averaged over all orientations:

$$\frac{\mathrm{d}\sigma_\mathrm{p}}{\mathrm{d}\Omega}(\mathbf{H}') = \frac{n_\mathrm{c}}{H^2}\int \frac{\mathrm{d}\sigma}{\mathrm{d}\Omega}(\mathbf{H}') R'(|\mathbf{H}'| - |\mathbf{H}_0|)\,\mathrm{d}\mathbf{H}', \quad (4.2.8.11)$$

where n_c is number of crystallites in the sample; this averaged cross section enters the relevant expressions for the convolution product with the resolution function.

A general intensity expression may be written as (Boysen, 1985)

$$I_n(H_0) = P \sum_T m(T) A_n \Phi_n(H_0, T). \quad (4.2.8.12)$$

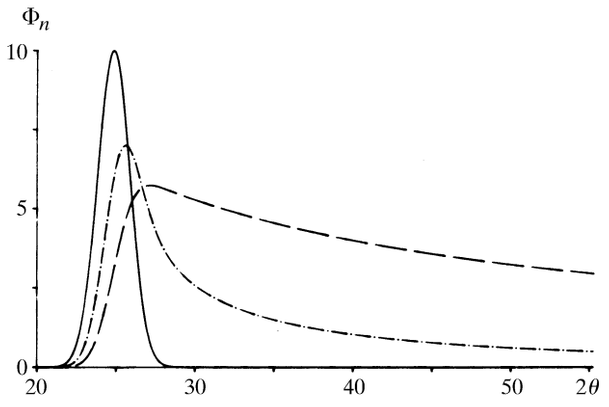

Fig. 4.2.8.2. Line profiles in powder diffraction for diffuse peaks (full line), continuous streaks (dot–dash lines) and continuous planes (broken lines). For explanation see text.

P denotes a scaling factor that depends on the instrumental luminosity, T is the shortest distance to the origin of the reciprocal lattice, $m(T)$ is the corresponding symmetry-induced multiplicity, A_n contains the structure factor of the structural units and the type of disorder, and Φ_n describes the characteristic modulation of the diffuse phenomenon of dimension n in the powder pattern. These expressions are given below with the assumption of Gaussian line shapes of width D for the narrow extension(s). The formulae depend on a factor $M = A_{1/2}(4k_1^2 - H_0^2)/(32\ln 2)$, where $A_{1/2}$ describes the dependence of the Bragg peaks on the instrumental parameters U, V and W (see Caglioti *et al.*, 1958),

$$A_{1/2}^2 = U\tan^2\theta + V\tan\theta + W, \qquad (4.2.8.13)$$

and $k_1 = 1/\lambda$.

(*a*) *Isotropic diffuse peak around T*

$$\Phi_0 = [2\pi(M^2 + D^2)]^{-1/2}(1/T^2) \times \exp\{-(H_0 - T)^2/2(M^2 + D^2)\}. \qquad (4.2.8.14)$$

The moduli $|\mathbf{H}_0|$ and T enter the exponential, *i.e.* the variation of $d\sigma/d\Omega$ along $|\mathbf{H}_0|$ is essential. For broad diffuse peaks ($M \ll D$) the angular dependence is due to $1/T^2$, *i.e.* proportional to $1/\sin^2\theta$. This result is valid for diffuse peaks of any shape.

(*b*) *Diffuse streak*

$$\Phi_1 = [2\pi(M^2 + D^2)]^{-1/2} \int_{-\infty}^{\infty} (T^2 + H^2)^{-1/2} \times \exp\{-H_0 - (T^2 + H^2)^{1/2}/2(M^2 + D^2)\}\,dH. \qquad (4.2.8.15)$$

The integral has to be evaluated numerically. If $(M^2 + D^2)$ is not too large, the term $1/(T^2 + H^2)$ varies only slowly compared to the exponential term and may be kept outside the integral, setting it approximately to $1/H_0^2$.

(*c*) *Diffuse plane (with $R^2 = H_x^2 + H_y^2$)*

$$\Phi_2 = (M^2 + D^2)^{-1/2} \int R^2/(T^2 + R^2) \times \exp\{-H_0 - (T^2 + R^2)^{1/2}/2(M^2 + D^2)\}\,dR. \qquad (4.2.8.16)$$

With the same approximation as in (*b*) the expression may be simplified to

$$\Phi_2 = \pi/H_0[1 - \mathrm{erf}\{(T - H_0)/[2(M^2 + D^2)]^{1/2}\} + 1/H_0^2[2\pi(M^2 + D^2)]^{1/2} \times \exp\{-(H_0 - T)^2/2(M^2 + D^2)\}]. \qquad (4.2.8.17)$$

(*d*) *Slowly varying diffuse scattering in three dimensions*

Φ_3 = constant. Consequently, the intensity is directly proportional to the cross section. The characteristic functions Φ_0, Φ_1 and Φ_2 are shown in Fig. 4.2.8.2 for equal values of T and D. Note the relative peak shifts and the high-angle tail.

4.2.8.3. Total diffraction pattern

As mentioned in Section 4.2.7.3.2, the atomic pair-distribution function (PDF), which is classically used for the analysis of the atomic distributions in liquids, melts or amorphous samples, can also be used to gain an understanding of disorder in crystals. The PDF is the Fourier transform of the total scattering. The measurement of total scattering is basically similar to recording X-ray or neutron powder patterns. The success of the method depends, however, decisively on various factors: (i) The availability of a large data set, *i.e.* reliable intensities up to high H values, in order to get rid of truncation ripples, which heavily influence the interpretation. Currently, values of $H_{\max}$ of more than 7 Å^{-1} can be achieved either with synchrotron X-rays [at the European Synchrotron Radiation Facility (ESRF) or Cornell High Energy Synchrotron Source (CHESS)] or with neutrons from reactors (*e.g.* instrument D4 at the ILL) and spallation sources [at ISIS or at LANSCE (instrument NPDF)]. (ii) High H resolution. (iii) High intensities, in particular at high H values. (iv) Low background of any kind which does not originate from the sample. High-quality intensities are therefore to be extracted from the raw data by taking care of an adequate absorption correction, correction of multiple-scattering effects, separation of inelastically scattered radiation (*e.g.* Compton scattering) and careful subtraction of 'diffuse' background which is not the 'true' diffuse scattering from the sample. These conditions are in practice rather demanding. A further detailed discussion is beyond the scope of this chapter, but a more thorough discussion is given, *e.g.*, by Egami (2004), and some examples are given by Egami & Billinge (2003).

References

Adlhart, W. (1981). *Diffraction by crystals with planar domains*. *Acta Cryst.* A**37**, 794–801.

Amorós, J. L. & Amorós, M. (1968). *Molecular Crystals: Their Transforms and Diffuse Scattering*. New York: John Wiley.

Arndt, U. W. (1986*a*). *X-ray position sensitive detectors*. *J. Appl. Cryst.* **19**, 145–163.

Arndt, U. W. (1986*b*). *The collection of single crystal diffraction data with area detectors*. *J. Phys. (Paris) Colloq.* **47**(C5), 1–6.

Aroyo, M. I., Boysen, H. & Perez-Mato, J. M. (2002). *Inelastic neutron scattering selection rules for phonons: application to leucite phase transitions*. *Appl. Phys. A*, **74**, S1043–S1048.

Axe, J. D. (1980). *Debye–Waller factors for incommensurate structures*. *Phys. Rev. B*, **21**, 4181–4190.

Bardhan, P. & Cohen, J. B. (1976). *X-ray diffraction study of short-range-order structure in a disordered Au_3Cu alloy*. *Acta Cryst.* A**32**, 597–614.

Bauer, G., Seitz, E. & Just, W. (1975). *Elastic diffuse scattering of neutrons as a tool for investigation of non-magnetic point defects*. *J. Appl. Cryst.* **8**, 162–175.

Bauer, G. S. (1979). *Diffuse elastic neutron scattering from nonmagnetic materials*. In *Treatise on Materials Science and Technology*, Vol. 15, edited by G. Kostorz, pp. 291–336. New York: Academic Press.

Berthold, T. & Jagodzinski, H. (1990). *Analysis of the distribution of impurities in crystals by anomalous X-ray scattering*. *Z. Kristallogr.* **193**, 85–100.

Bessière, M., Lefebvre, S. & Calvayrac, Y. (1983). *X-ray diffraction study of short-range order in a disordered Au_3Cu alloy*. *Acta Cryst.* B**39**, 145–153.

Beyeler, H. U., Pietronero, L. & Strässler, S. (1980). *Configurational model for a one-dimensional ionic conductor*. *Phys. Rev. B*, **22**, 2988–3000.